Scientific Research Publishing

Computational Chemistry, 2022, 10, 53-70
https://www.scirp.org/journal/cc
ISSN Online: 2332-5984
ISSN Print: 2332-5968

Catechin and Epicatechin. What's the More Reactive?

Essoh Akpa Eugène, N'guessan Boka Robert, Adenidji Ganiyou, Yapo Kicho Denis, Adjou Ané, Bamba El Hadji Sawaliho*

Laboratoire de Constitution et de Réaction de la Matière, UFR SSMT, Université Félix Houphouët-Boigny, Abidjan, Côte d'Ivoire
Email: *bame1901@usherbrooke.ca

How to cite this paper: Eugène, E.A., Robert, N.B., Ganiyou, A., Denis, Y.K., Ané, A. and El Hadji Sawaliho, B. (2022) Catechin and Epicatechin. What's the More Reactive? *Computational Chemistry*, **10**, 53-70.
https://doi.org/10.4236/cc.2022.102003

Received: December 24, 2021
Accepted: March 8, 2022
Published: March 11, 2022

Abstract

Catechin and epicatechin are two isomeric flavonoids. Despite the vital properties highlighted by numerous scientific studies, very little data is available on the intrinsic reactivity of these compounds. To provide more details on the stability and reactivity of catechin and epicatechin, this study is performed by means of theoretical calculation methods. For this purpose, geometry optimizations and frequency calculations at the B3LYP/6-31 + G (d, p) level of theory has been carried out and Natural Bond Orbital (NBO) analysis and VEDA (Vibrational Energy Distribution Analysis). The geometric and energy parameters and NBO analysis show that catechin appears more stable than epicatechin. The hydroxyl group position on the ring C of the catechol structure represents a factor that influences this relative stability. The global and local reactivity parameters reveal that epicatechin becomes more reactive than catechin. They indicate that their hydroxyl groups correspond to their most receptive sites. Fukui indices, VEDA and acidity study establish that O_{28}–H_{29} remains the most reactive.

Keywords

Catechin, Epicatechin, NBO, Acidity, DFT, Normal Modes

1. Introduction

Catechin and epicatechin are two isomeric flavanols. They differ from the R and S configuration linked to the two asymmetric carbons of 2-phenyl-3-chromanol (**Figure 1**) [1] [2] [3] [4]. In **Figure 1**, each ball represents an atom. Red is oxygen. A white ball illustrates the carbon. A small one describes hydrogen. Catechin and epicatechin are widespread in the plant kingdom through fruits such as grapes, apples and too many manufactured products such as wine, chocolate,

and tea [2] [5]. With the consumption of these foods, humans benefit from antioxidant properties [6] [7] [8] [9] [10]. These delay cell damage and combat certain chronic diseases including cardiovascular and neurodegenerative diseases ones [6] [7] [11] [12] [13] [14]. These molecules also possess anti-cancer, anti-inflammatory and anti-viral properties [15] [16] [17] [18]. The wide spectrum of polyphenols' biological activities gives them a great importance in therapeutic processes. Besides, only 2% of these alcohols consumed reach the plasma. This underperformance thus represents a problem of bioavailability [19]. Increasing their proportion in this organism would make them much more efficacious. For better control and improvement of polyphenols' therapeutic effects, it's advisable to discover ways to grow their concentration in plasma. The development of medicines incorporating polyphenols would be an asset in providing effective remedies for these illnesses that ruin human populations. Tests to manufacture catechin-specific anti-inflammatory drugs weren't as conclusive as expected. The reasons are related to the failures of the very limited clinical tests because of their stability, their short half-life in the plasma and their low bioavailability [20] [21].

The properties exhibited by catechin and epicatechin emanate from their many hydroxyl groups [22]. The aromatic rings and their OH associated makes it possible to build several types of interactions. These permit polyphenols to scavenge hydroxyl radicals, inhibit reactions such as lipid peroxidation and

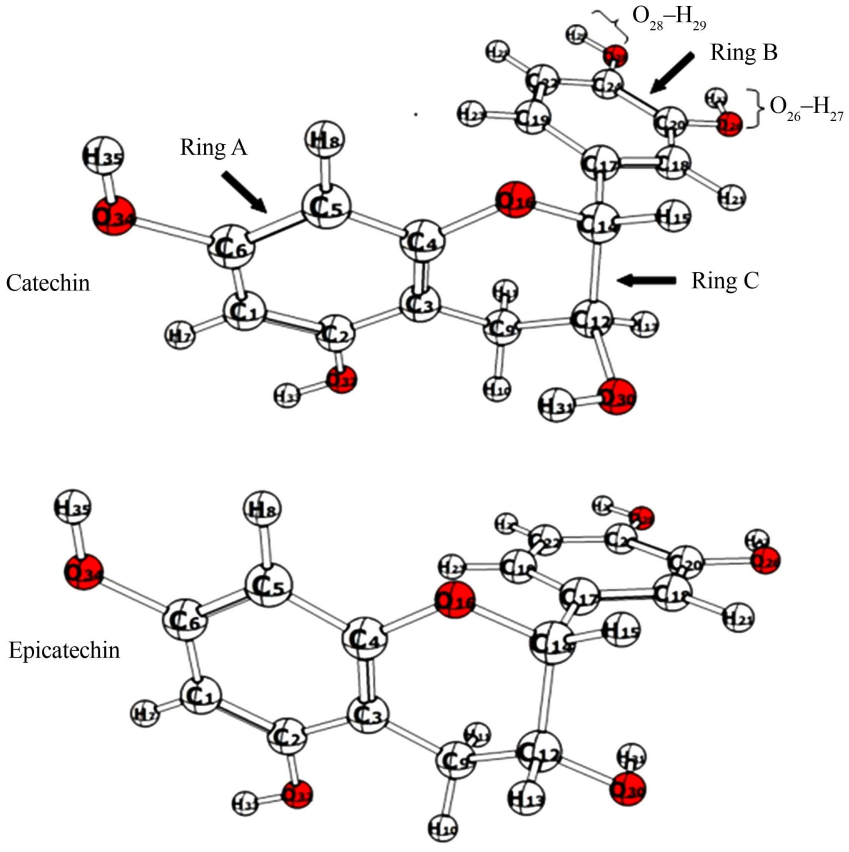

Figure 1. Structure of Catechin and Epicatechin.

prevent oxidation reactions. This process happens in a state of transition [22]; the latter promotes the occupation of their specific molecular orbitals [23]. These foster some CHO bond at three centres. However, despite the large number of studies on the biological mechanisms explaining the beneficial effects of polyphenols on human health, few quantitative data are available on the polyphenol's reactivity. This research aims to fill this gap through the following question:

Which isomer is the most reactive between catechin and epicatechin?

Its response fulfills the gap in numerical data relating to the reactivity of the two compounds. But it's difficult to identify all the factors involved in the instability of the two isomers. To correct this shortcoming, the work wants to address another question:

What are the most receptive sites of isomers?

The research plans to suggest avenues that will contribute to a better integration of molecular interactions and biological activities. It assimilates catechin and epicatechin to a polyphenol model. It evaluates their reactivity using physical and chemical quantities. These include the energy, infrared (IR) and ultraviolet (UV) spectroscopic parameters. They incorporate electronic properties such as the HOMO (High Occupied Molecular Orbital)-LUMO (Lowest Unoccupied Molecular Orbital) energy gap, chemical hardness and chemical potential. They comprise molecular electrostatic potential (MEP) and Fukui indices. These analyze the local and global reactivity. Furthermore, the acidity potential (pKa) specifies that of each hydroxyl group. Natural Bond Orbital (NBO) analysis allows following charge transfer and intramolecular interactions in catechin and epicatechin. This article discusses the calculations relating to these parameters. Previously, it presented the method and the material used to obtain them.

2. Materials and Methods

This part includes the descriptors of global and local reactivity. It explains those of acidity. It describes how to assess load transfers using NBO analysis. For the moment, it specifies the method of calculations. The bond lengths, the bond angles and the standard dihedral angle constitute the initial geometrical parameters. The geometry optimizations and the frequency calculations were carried out with the Density Functional Theory (DFT) method at the B3LYP/6-31 + G(d, p) level of theory [24] in gas and aqueous phases.

2.1. Calculation Method

The CPCM (Conductor-like Polarizable Continuum Model) calculation simulates the physiological environment. All calculations were performed with the GAUSSIAN 09 software [25]. Frequency calculations verify local and global minima. TD-DFT method permits to analyze the electron transitions in the ultraviolet (UV) range. The research determines the energies of the frontier molecular orbitals including the highest occupied one (HOMO) and the lowest unoccu-

pied one (LUMO). It uses NBO calculation [26] examining the NBO. Gaussian's calculations provide access to the frontier orbitals of a molecule. Their HOMO and LUMO contribute interpreting the reactivity of a molecule [27] [28].

2.2. Global Reactivity Descriptors

The energies of these two frontier orbitals lead to the determination of several reactivity parameters. According to Koopmans theorem [29], the ionization energy I and the electronic affinity A are directly related to the energy of the HOMO and the LUMO respectively.

$$I = -E_{\text{HOMO}} \tag{1}$$

$$A = -E_{\text{LUMO}} \tag{2}$$

The chemical electron potential μ and chemical hardness η are defined in terms of ionization energy and electron affinity [30]:

$$\mu = \frac{A+I}{2} \tag{3}$$

$$\eta = \frac{I-A}{2} \tag{4}$$

Also, global index of electrophilicity ω, introduced by Parr [31], is defined by the following formula:

$$\omega = \mu^2 / \eta \tag{5}$$

Local reactivity index is also accessible by calculation. While the global reactivity parameters evaluate that of a molecule, Fukui [32] introduces indices (Fukui parameters) to describe the reactivity of each atom.

2.3. Local Reactivity Descriptors

These parameters denote either a nucleophilic attack (f_k^+), an electrophilic attack (f_k^-), or a radical attack (f_k^0). The following equations [33] help to determine them:

$$f_k^+ = q_k(N+1) - q_k(N) \tag{6}$$

$$f_k^- = q_k(N) - q_k(N-1) \tag{7}$$

$$f_k^0 = \left[q_k(N+1) - q_k(N-1)\right]/2 \tag{8}$$

With

$q_k(N)$: the electron population of atom k in the neutral molecule.

$q_k(N+1)$: the electron population of atom k in the cationic molecule.

$q_k(N-1)$: the electron population of atom k in the anionic molecule.

The acidity represents an important parameter to integrate the intermolecular interactions. The calculations give access to the pKa.

2.4. Acidity

Catechin and epicatechin represent polyphenols with both five hydroxyl groups.

They're therefore likely to exchange one or more protons with other molecules, either during hydrogen bonding interactions or "antiradical" mechanisms [34]. The pKa of each hydroxyl group evaluates the proton transfer reactions between catechin and epicatechin and additional molecules. It helps classifying their acidity. The thermodynamic cycle below allows calculating it by considering the effect of solvation due to the presence of H_2O [35].

The free energy of solvation ΔG_{sol} becomes:

$$\Delta G_{sol} = \Delta G_g + \Delta G_{solv}\left(A^-\right) + \Delta G_{solv}\left(H_3O^+\right) - \Delta G_{solv}\left(AH\right) - \Delta G_{solv}\left(H_2O\right) \quad (9)$$

The value of $\Delta G_{solv}\left(H_3O^+\right)$ equals −110.2 kcal/mol. Pliego and Riveros [36] determined it experimentally.

$$\text{pKa} = \frac{\Delta G_{sol}}{1.364} - \log\left[H_2O\right] \quad (10)$$

where $[H_2O]$ = 55.5 M. However, since the free energy of the hydronium ion constitutes a source of error. According to Pliego [35], the corrected formula for pKa is written as follows. On the other hand, this calculation of Pka leads to the NBO analysis.

$$\text{pKa}\left(\text{corrected}\right) = \text{pKa} - 4.54 \quad (11)$$

2.5. NBO Analysis

NBO analysis [26] evaluates the charge transfer properties in molecules. It provides a deep understanding of intramolecular and intermolecular orbital interactions between occupied NBO donors and empty NBO acceptors [37] [38]. The charge transfer involves delocalization of electrons from an electron donor site Lewis-type orbital: lone pairs (n), natural bond (σ and π) to an electron acceptor one (anti-Lewis orbital: σ^* and π^*). This electron delocalization is with a decrease in the donor electronic density and an increase in the acceptor one. For each donor NBO (i) and acceptor NBO (j), the electron delocalization $i \rightarrow j$ is evaluated by the stabilization energy $E^{(2)}$ using second-order perturbation theory [39]. This latter is expressed as:

$$E^{(2)} = \Delta E_{ij} = q_i \frac{F\left(i,j\right)^2}{\varepsilon_i - \varepsilon_j} \quad (12)$$

where q_i denotes the electronic density in the donor orbital, $F\left(i,j\right)$ designs a non-diagonal element of the Fock matrix, ε_i and ε_j correspond to the energies of the occupied i and empty j orbitals respectively. The higher $E^{(2)}$, the more redistribution of electrons between donor and acceptor confers stability. This affirmation introduces the presentation of the results and their analysis.

3. Results and Discussion

This section discusses those related to indicators of global and local responsiveness. Its analysis concerns acidity and NBO comprise results of calcula-

tions associated with spectral quantities. Catechin or epicatechin is composed of 35 atoms. Vibration mode analysis suggests 99 normal vibrations for both molecules.

3.1. Spectroscopic Parameters

These vibrations are divided into 34 stretching, 33 deformations and 32 torsions. The 34 stretching is repartitioned into five O–H, nine C–H, 13 C–C and seven C–O. This agrees with the structure of the two molecules (**Figure 1**). The analysis of the potential energy distribution (PED) by VEDA can efficiently assign the calculated normal modes of vibration. **Table 1** presents the O–H elongation vibration frequencies of catechin and epicatechin. It indicates that the catechin and epicatechin O–H elongation frequencies vary from 3788 to 3845 cm^{-1}. These agree with the experimental values of the O–H bonds of aromatic rings [40].

The first three O–H elongation frequencies stay at 3845 cm^{-1}, 3833 cm^{-1}, and 3830 cm^{-1} correspond to $\nu_{O_{28}-H_{28}}$, $\nu_{O_{32}-H_{33}}$, and $\nu_{O_{34}-H_{35}}$, respectively, of the two molecules. Their intensities are approximately the same. The ranking of the –H bonds by their elongation frequencies is:

$\nu_{O_{28}-H_{28}} > \nu_{O_{32}-H_{33}} > \nu_{O_{34}-H_{35}} > \nu_{O_{26}-H_{27}} > \nu_{O_{30}-H_{31}}$ for epicatechin and

$\nu_{O_{28}-H_{28}} > \nu_{O_{32}-H_{33}} > \nu_{O_{34}-H_{35}} > \nu_{O_{30}-H_{31}} > \nu_{O_{26}-H_{27}}$ for catechin. $\nu_{O_{30}-H_{31}}$ changes from 3803 cm^{-1} in catechin to 3788 cm^{-1} in epicatechin. Their intensities of this vibration also change. They increase from 28.44 km/mole in the catechin to 61.35 km/mole. O_{30}–H_{31} is affected by the asymmetry of carbon C_{12}.

3.2. UV-Visible Spectral Analysis

The TD-DFT method at the level of the theory B3LYP/6-31 + G (d, p), in the gas phase evaluates the electron transitions of catechin or epicatechin in the ultraviolet and visible regions. It gives molecule excitation energy. This latter quantity permits comparing the reactivity of two molecules. Its higher value corresponds to the more stable compound. **Table 2** shows the results of the TD-DFT calculations. It displays the first three excited states of both molecules as presented in **Figure 2**.

Table 1. Vibrational frequencies (cm^{-1}), IR intensity (km/mol) and vibrational assignation (PED) of Catechin and Epicatechin.

Catechin			Epicatechin		
$\nu(cm^{-1})$	IR intensity	Vibrational assign. (PED)	$\nu(cm^{-1})$	IR intensity (km/mol)	Vibrational assignation
3845	86.99	$\nu_{O_{28}H_{29}}$ (100)	3844	87.95	$\nu_{O_{28}H_{29}}$ (100)
3833	68.90	$\nu_{O_{32}H_{33}}$ (100)	3833	67.91	$\nu_{O_{32}H_{33}}$ (100)
3830	67.31	$\nu_{O_{34}H_{35}}$ (100)	3830	66.91	$\nu_{O_{34}H_{35}}$ (100)
3803	28.44	$\nu_{O_{30}H_{31}}$ (100)	3789	86.13	$\nu_{O_{26}H_{27}}$ (94)
3788	118.71	$\nu_{O_{26}H_{27}}$ (100)	3788	61.35	$\nu_{O_{30}H_{31}}$ (94)

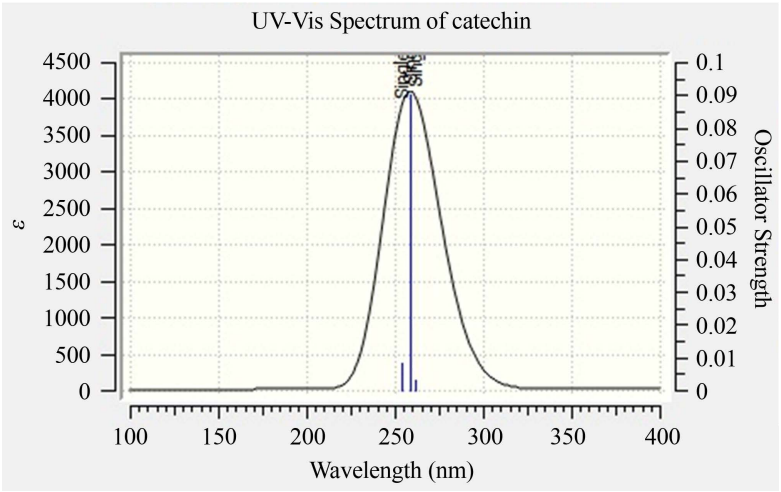

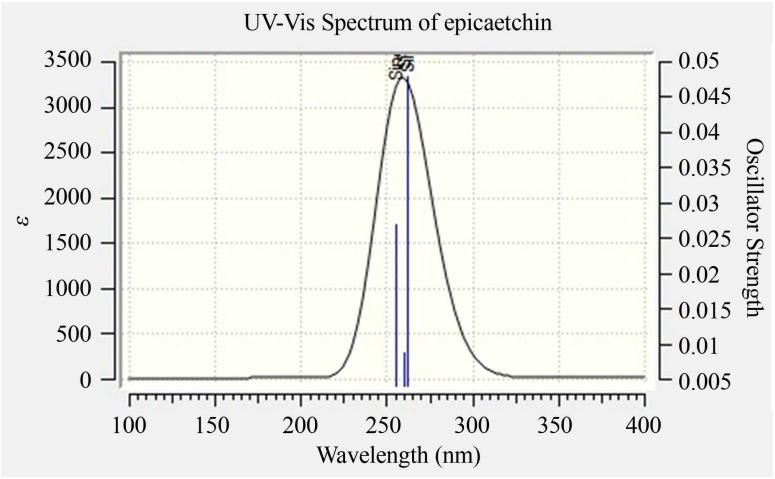

Figure 2. UV-visible spectra of catechin and epicatechin.

Table 2. Main transitions calculated for Catechin and Epicatechin.

	Excited State	ΔE (eV)	λ (nm)	f (a.u.)	Transition	Composition (%)
Catechin	First	4.7453	261.28	0.0032	HOMO → LUMO + 1	54.03
	Second	4.7851	259.11	0.0902	HOMO → LUMO	60.56
	Third	4.8871	253.70	0.0081	HOMO−1 → LUMO	50.35
Epicatechin	First	4.7355	261.82	0.0479	HOMO → LUMO	61.19
	Second	4.7650	260.20	0.0087	HOMO → LUMO + 1	44.24
	Third	4.8607	255.08	0.0269	HOMO−1 → LUMO	47.40

For epicatechin, the first excited state wavelength is 262 nm. This is the most intense excitation. Its main component refers to the HOMO → LUMO transition with a weight of 61%. Its excitation energy is 4.7355 eV. The second one relates to the band with a wavelength equals 260.20 nm. It associates with the HOMO − 2 → LUMO + 1 transition. Its excitation energy is 4.7453 eV. The latter is greater

than that of the first excited state. This result means that epicatechin is more reactive than catechin.

3.3. Global Reactivity Descriptors

To access the chemical reactivity of catechin or epicatechin, it's necessary to determine their molecular border orbital HOMO and LUMO [27]. More, the first orbitals can explain the physical and chemical properties of molecules [23]. Here, they help to provide insight into intramolecular charge transfers; an electron-rich HOMO orbital acts as a donor; an electron-poor LUMO functions as an acceptor. **Figure 3** and **Figure 4** illustrate the HOMO − 3 to LUMO + 3 boundary orbitals of catechin and epicatechin. These molecular orbitals have a π character.

For HOMO, the π character is distributed over all the catechin and epicatechin. This means that the delocalization of electrons occurs through the molecules of catechin and epicatechin. Unlike LUMO, the π character of these molecules is concentrated on the B-cycle with a residual contribution of its oxygen atoms. The global reactivity indices are presented in **Table 3**. The smaller the energy gap (ΔE) between HOMO and LUMO is, the more reactive is the molecule [27]. The energy gap of epicatechin (5.347 eV) is the lowest. It indicates that this molecule is most receptive. The global electrophilicity indices ω confirms this observation. Its epicatechin's value is slightly higher than those of catechin. The epicatechin is more able to acquire electronic charges. The chemical hardness of epicatechin η (2.674 eV) is lower than that of catechin (2.720 eV). The epicatechin is softer than catechin. The Fukui indices f_k^+, f_k^-, and f_k^0 represents the local reactivity descriptors.

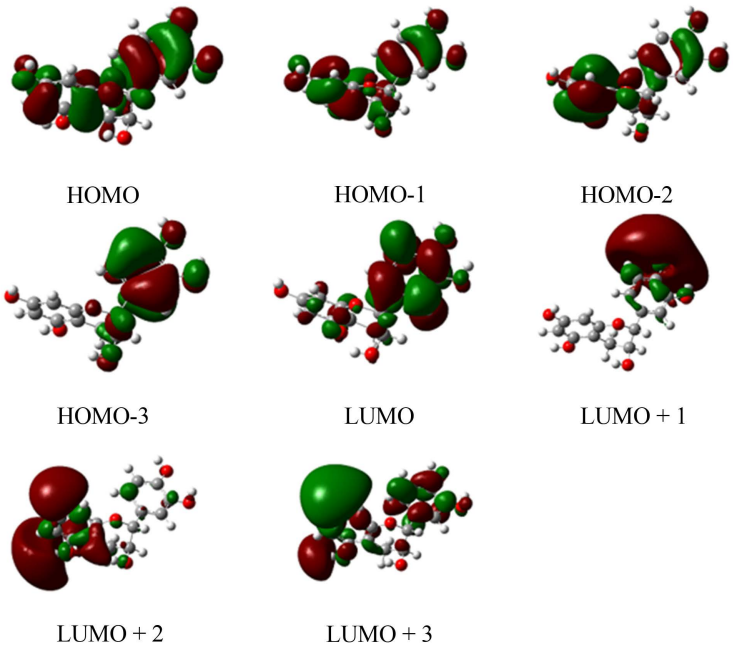

Figure 3. Frontier orbitals of the catechin's main calculated transitions.

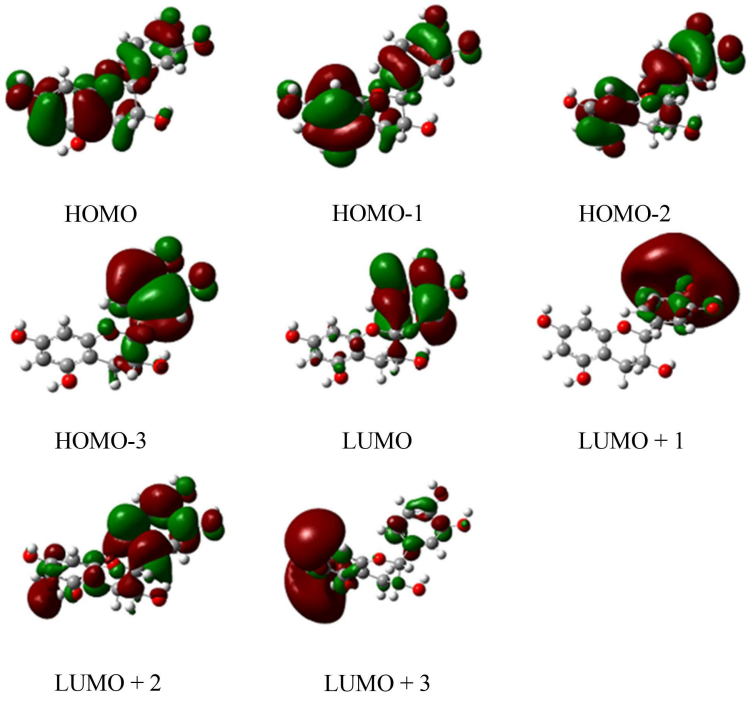

Figure 4. Frontier orbitals of the epicatechin's main calculated transitions.

Table 3. Global reactivity parameters of catechin and epicatechin.

molecules	E_{HOMO} (eV)	E_{LUMO} (eV)	ΔE (eV)	η (eV)	μ (eV)	ω (eV)
Catechin	−6.054	−0.614	5.440	2.720	−3.334	2.0433
Epicatechin	−6.008	−0.661	5.347	2.674	−3.335	2.0791

3.4. Local Reactivity Descriptors

Fukui indices are used to assess the reactivity of atoms or functional groups (nucleophilic or electrophilic attack site) of a molecule [33]. This work is based on a natural population analysis (NPA) in gas and aqueous phase to estimate the electron population [41]. This leads to the Fukui indices, reported in **Tables 4-6**. The Molecular Electrostatic Potential (MEP) map displays the electron density of a molecule as a function of colour. It constitutes a descriptor of the local reactivity for a molecule. Colours indicate the electron density of areas of the molecule [42]. A red region illustrates an electron-rich site. A blue zone describes an electron-poor site. A green area is a neutral site. **Figure 5** gives the plots of the catechin and epicatechin electrostatic potential.

These tables data show that the highest f_k^+ values in both the aqueous and gas phases link to the hydrogen atoms H_{27}, H_{29}, H_{31}, H_{33}, and H_{35} of catechin and epicatechin. These constitute the preferential sites of nucleophilic attack. On the other hand, some are favoured on the oxygen atoms and the carbon atoms of the aromatic rings. The properties are preserved when the molecule passing from the gas phase of the aqueous phase.

Table 4. Global reactivity parameters of catechin and epicatechin (atoms 1 to 12).

	Epicatechin				Catechin			
	Gas phase		Aqueous phase		Gas phase		Aqueous phase	
Atom	f_k^+	f_k^-	f_k^+	f_k^-	f_k^+	f_k^-	f_k^+	f_k^-
C_1	−0.200	0.085	−0.195	0.154	−0.132	0.064	−0.192	0.062
C_2	0.172	−0.020	0.174	−0.150	0.256	−0.012	0.178	−0.008
C_3	−0.092	0.141	−0.095	−0.002	−0.094	0.159	−0.103	0.136
C_4	0.175	0.025	0.167	−0.166	0.174	0.014	0.166	0.012
C_5	−0.191	−0.005	−0.192	0.207	−0.148	0.000	−0.189	0.007
C_6	0.168	0.055	0.168	−0.170	0.195	0.061	0.168	0.054
H_7	0.125	0.026	0.131	−0.112	0.134	0.027	0.131	0.016
H_8	0.127	0.025	0.132	−0.115	0.134	0.024	0.132	0.017
H_9	−0.253	−0.027	−0.254	0.236	−0.243	−0.029	−0.254	−0.022
H_{10}	0.143	0.026	0.142	−0.128	0.144	0.029	0.142	0.021
H_{11}	0.124	0.023	0.129	−0.122	0.135	0.024	0.137	0.022
H_{12}	0.027	−0.003	0.025	−0.030	0.033	−0.002	0.030	−0.001

Table 5. Global reactivity parameters of catechin and epicatechin (atoms 13 to 24).

	Epicatechin				Catechin			
	Gas phase		Aqueous phase		Gas phase		Aqueous phase	
Atom	f_k^+	f_k^-	f_k^+	f_k^-	f_k^+	f_k^-	f_k^+	f_k^-
H_{13}	0.129	0.015	0.133	−0.118	0.130	0.015	0.133	0.011
H_{14}	0.027	−0.013	0.019	−0.027	0.029	−0.016	0.027	−0.015
H_{15}	0.137	0.030	0.143	−0.124	0.143	0.028	0.157	0.026
O_{16}	−0.267	0.058	−0.273	0.267	−0.270	0.042	−0.274	0.038
C_{17}	−0.033	0.042	−0.065	0.040	−0.011	0.037	0.061	0.062
C_{18}	−0.148	0.000	−0.188	0.144	−0.099	−0.003	0.042	−0.001
C_{19}	−0.122	0.052	−0.101	0.121	−0.116	0.055	−0.133	0.075
C_{20}	0.146	0.063	0.138	−0.134	0.155	0.066	0.136	0.082
H_{21}	0.140	0.023	0.149	−0.128	0.136	0.021	0.139	0.019
C_{22}	−0.159	−0.007	−0.183	0.152	−0.025	−0.005	0.080	−0.003
H_{23}	0.131	0.005	0.140	−0.129	0.135	0.008	0.139	0.015
C_{24}	0.112	0.064	0.105	−0.125	0.246	0.064	0.343	0.080

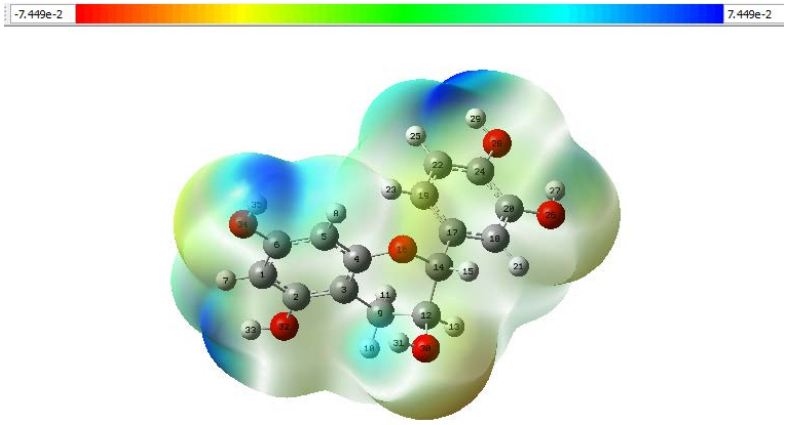

catechin

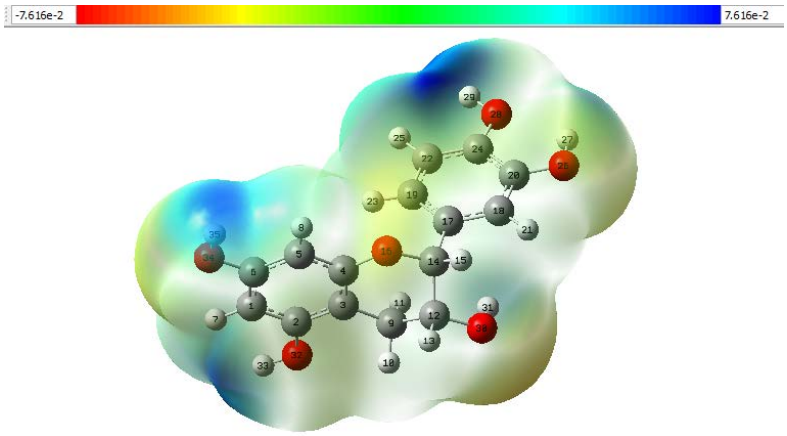

epicatechin

Figure 5. Molecular electrostatic potential of Catechin and Epicatechin.

Table 6. Global reactivity parameters of catechin and epicatechin (atoms 25 to 35).

	Epicatechin				Catechin			
	Gas phase		Aqueous phase		Gas phase		Aqueous phase	
Atom	f_k^+	f_k^-	f_k^+	f_k^-	f_k^+	f_k^-	f_k^+	f_k^-
H_{25}	0.119	0.023	0.148	−0.127	0.124	0.024	0.139	0.020
O_{26}	−0.350	0.064	−0.355	0.368	−0.342	0.068	−0.351	0.072
H_{27}	0.263	0.016	0.273	−0.267	0.277	0.017	0.284	0.014
O_{28}	−0.376	0.049	−0.364	0.374	−0.295	0.049	−0.318	0.060
H_{29}	0.256	0.020	0.278	−0.269	0.377	0.021	0.380	0.017
O_{30}	−0.379	0.018	−0.393	0.401	−0.381	0.019	−0.397	0.011
H_{31}	0.249	0.005	0.256	−0.254	0.254	0.002	0.259	0.003
O_{32}	−0.360	0.021	−0.363	0.383	−0.311	0.025	−0.362	0.020
H_{33}	0.257	0.020	0.268	−0.258	0.315	0.020	0.268	0.010
O_{34}	−0.356	0.061	−0.365	0.365	−0.343	0.064	−0.364	0.052
H_{35}	0.257	0.021	0.267	−0.253	0.282	0.021	0.266	0.012

This map indicates that the hydroxyl groups O_{28}–H_{29}, O_{32}–H_{33}, and O_{34}–H_{35}, are more depleted in electrons than those of O_{30}–H_{31}, O_{26}–H_{27} and of the different C_i–H_j bonds. These hydrogen atoms of the O_i–H_j hydroxyl groups and C_i–H_j bonds of catechin and epicatechin are sites conducive to nucleophilic attack on the following decreasing order of reactivity : O_{28}–H_{29} > O_{32}–H_{33} > O_{34}–H_{35} > O_{26}–H_{27} > O_{30}–H_{31} > C_i–H_j. The regions of the oxygen atoms and the aromatic rings are, on the other hand, favourable sites for electrophilic attacks.

3.5. Acidity

Table 7 shows the theoretical values of pKa for each hydroxyl group of the catechin and its isomer. This statistic varies from 6.77 to 21.77 for catechin and from 6.77 to 21.70 for epicatechin. The pka of the hydroxyl group's O_{32}–H_{33}, O_{34}–H_{35} and O_{26}–H_{27} are respectively 9.92, 10.47, 11.47 for catechin. For epicatechin, they're 10.56, 11.21, 1171. These values are close to the pka experimental value of the phenol's hydroxyl; the latter is equal to 9.95 [43]. The pKa values of the hydroxyl group O_{28}–H_{29} are 7.53 in catechin and 6.77 in epicatechin. These values remain inferior to 9.85. Therefore, the hydroxyl group O_{28}–H_{29} of catechin or epicatechin is more acidic than the phenol's hydroxyl group and those of catechin or epicatechin. The difference between the pKa of the hydroxyl group O_{30}–H_{31} and that of the phenol is great. It shows that the hydroxyl group isn't on an aromatic ring. Its acidic character is very weak compared to the other hydroxyl groups of catechin and epicatechin. The hydroxyl group acidity becomes: O_{28}–H_{29} > O_{32}–H_{33} > O_{34}–H_{35} > O_{26}–H_{27} > O_{30}–H_{31}. The hydroxyl groups O_{28}–H_{29}, O_{32}–H_{33}, O_{34}–H_{35} are much more acidic. They're more favourable to the anti-radical processes than the hydroxyl groups O_{26}–H_{27} or O_{30}–H_{31}.

3.6. NBO Analysis

Table 8 and Table 9 collate the second-order perturbation energies $E^{(2)}$, the electron density (ED), the energy difference $E(j) - E(i)$ of the donor NBO (i) and of the acceptor NBO (j) related to catechin and epicatechin. They show their elements of the Fock matrix $F(i, j)$. These results indicate that for catechin and epicatechin, the main interactions are of two types. They're intramolecular interactions of the types $\pi^{(2)}_{C\alpha-C\beta} \rightarrow \pi^{*(2)}_{C\gamma-C\delta}$ and $n^{(2)}_{O\varepsilon} \rightarrow \pi^{*(2)}_{C\gamma-C\delta}$ where $\pi^{(2)}_{C\alpha-C\beta}$, $n^{(2)}_{O\varepsilon}$,

Table 7. pKa values of catechin and epicatechin.

hydroxyl group	pKa	
	Catechin	Epicatechin
O_{30}–H_{31}	21.77	21.70
O_{32}–H_{33}	9.92	10.56
O_{34}–H_{35}	10.47	11.21
O_{26}–H_{27}	11.78	11.71
O_{28}–H_{29}	7.53	6.77

Table 8. The catechin's NBO parameters.

Catechin						
Donor		Acceptor		$E^{(2)}$ (kcal/mol)	$E(j) - E(i)$ (a.u.)	$F(i, j)$ (a.u.)
Orbital	ED (e)	Orbital	ED (e)			
$\pi^{(2)}_{C1-C2}$	1.71091	$\pi^{*(2)}_{C3-C4}$	0.42126	12.52	0.29	0.055
$\pi^{(2)}_{C1-C2}$	1.71091	$\pi^{*(2)}_{C5-C6}$	0.40712	25.81	0.28	0.079
$\pi^{(2)}_{C3-C4}$	1.69169	$\pi^{*(2)}_{C1-C2}$	0.40662	25.41	0.28	0.077
$\pi^{(2)}_{C3-C4}$	1.69169	$\pi^{*(2)}_{C5-C6}$	0.40712	12.88	0.28	0.055
$\pi^{(2)}_{C5-C6}$	1.71003	$\pi^{*(2)}_{C1-C2}$	0.40662	12.26	0.28	0.054
$\pi^{(2)}_{C5-C6}$	1.71003	$\pi^{*(2)}_{C3-C4}$	0.42126	24.64	0.29	0.078
$\pi^{(2)}_{C17-C19}$	1.68580	$\pi^{*(2)}_{C18-C20}$	0.37976	18.65	0.27	0.065
$\pi^{(2)}_{C17-C19}$	1.68580	$\pi^{*(2)}_{C22-C24}$	0.39742	19.91	0.27	0.066
$\pi^{(2)}_{C18-C20}$	1.67554	$\pi^{*(2)}_{C17-C19}$	0.36492	20.33	0.30	0.070
$\pi^{(2)}_{C18-C20}$	1.67554	$\pi^{*(2)}_{C22-C24}$	0.39742	19.32	0.28	0.067
$\pi^{(2)}_{C22-C24}$	1.70705	$\pi^{*(2)}_{C17-C19}$	0.36492	17.47	0.31	0.066
$\pi^{(2)}_{C22-C24}$	1.70705	$\pi^{*(2)}_{C18-C20}$	0.37976	18.42	0.29	0.067
$n^{(2)}_{O16}$	1.84295	$\pi^{*(2)}_{C3-C4}$	0.42126	29.69	0.34	0.096
$n^{(2)}_{O26}$	1.87435	$\pi^{*(2)}_{C18-C20}$	0.37976	27.75	0.35	0.094
$n^{(2)}_{O28}$	1.89789	$\pi^{*(2)}_{C22-C24}$	0.39742	24.07	0.36	0.090
$n^{(2)}_{O32}$	1.87678	$\pi^{*(2)}_{C1-C2}$	0.40662	28.50	0.35	0.096
$n^{(2)}_{O34}$	1.87887	$\pi^{*(2)}_{C5-C6}$	0.40712	28.65	0.35	0.097

Table 9. The epicatechin's NBO parameters.

Epicatechin						
Donor		Acceptor		$E^{(2)}$ (kcal/mol)	$E(j) - E(i)$ (a.u.)	$F(i, j)$ (a.u.)
Orbital	ED (e)	Orbital	ED (e)			
$\pi^{(2)}_{C1-C2}$	1.71167	$\pi^{*(2)}_{C3-C4}$	0.41979	12.40	0.29	0.055
$\pi^{(2)}_{C1-C2}$	1.71167	$\pi^{*(2)}_{C5-C6}$	0.40740	25.74	0.28	0.079
$\pi^{(2)}_{C3-C4}$	1.68796	$\pi^{*(2)}_{C1-C2}$	0.40993	25.95	0.28	0.078
$\pi^{(2)}_{C3-C4}$	1.68796	$\pi^{*(2)}_{C5-C6}$	0.40740	13.01	0.28	0.055
$\pi^{(2)}_{C5-C6}$	1.70973	$\pi^{*(2)}_{C1-C2}$	0.40993	12.28	0.28	0.054
$\pi^{(2)}_{C5-C6}$	1.70973	$\pi^{*(2)}_{C3-C4}$	0.41979	24.71	0.29	0.078

Continued

$\pi^{(2)}_{C17-C19}$	1.67829	$\pi^{*(2)}_{C18-C20}$	0.38557	19.08	0.27	0.065
$\pi^{(2)}_{C17-C19}$	1.67829	$\pi^{*(2)}_{C22-C24}$	0.40148	20.07	0.27	0.067
$\pi^{(2)}_{C18-C20}$	1.66656	$\pi^{*(2)}_{C17-C19}$	0.37121	20.25	0.29	0.070
$\pi^{(2)}_{C18-C20}$	1.66656	$\pi^{*(2)}_{C22-C24}$	0.40148	19.61	0.28	0.067
$\pi^{(2)}_{C22-C24}$	1.69886	$\pi^{*(2)}_{C17-C19}$	0.37121	17.87	0.30	0.067
$\pi^{(2)}_{C22-C24}$	1.69886	$\pi^{*(2)}_{C18-C20}$	0.38557	18.56	0.29	0.067
$n^{(2)}_{O16}$	1.84377	$\pi^{*(2)}_{C3-C4}$	0.41979	29.65	0.34	0.097
$n^{(2)}_{O26}$	1.87363	$\pi^{*(2)}_{C18-C20}$	0.38557	27.66	0.34	0.093
$n^{(2)}_{O28}$	1.89676	$\pi^{*(2)}_{C22-C24}$	0.40148	24.13	0.36	0.090
$n^{(2)}_{O32}$	1.87803	$\pi^{*(2)}_{C1-C2}$	0.40993	28.25	0.35	0.096
$n^{(2)}_{O34}$	1.87952	$\pi^{*(2)}_{C5-C6}$	0.40740	28.50	0.35	0.096

$\pi^{*(2)}_{C\gamma-C\delta}$ are: Lewis π orbital of the $C\alpha=C\beta$ double bond, the lone pair 2 of the Oε atoms, anti-Lewis π orbital of the $C\gamma=C\delta$ double bond. α, β, γ, δ, ε are atomic numbers. In the aromatic ring A, the stabilization energies of the $\pi^{(2)}_{C1-C2}\rightarrow\pi^{*(2)}_{C5-C6}$, $\pi^{(2)}_{C3-C4}\rightarrow\pi^{*(2)}_{C1-C2}$ and $\pi^{(2)}_{C5-C6}\rightarrow\pi^{*(2)}_{C3-C4}$ interactions are 25, 81, 25.41, 24.64 kcal/mol respectively for catechin and 25.74, 25.95, 24.71 kcal/mol for epicatechin.

In aromatic ring B, for the same intramolecular interaction $\pi^{(2)}_{Ci-Cj}\rightarrow\pi^{*(2)}_{Cm-Cn}$, the maximum stabilization energy is equal to 20.33 kcal/mol for catechin and 20.25 kcal/mol for epicatechin. Thus, the aromatic ring B is less stable than of the A one. Regarding the $n^{(2)}_{Oi}\rightarrow\pi^{*(2)}_{Cm-Cn}$ interactions, the lowest stabilization energy is obtained with $n^{(2)}_{O28}\rightarrow\pi^{*(2)}_{C22-C24}$. For catechin, it's worthy 24.07 kcal/mol and 24.13 kcal/mol for epicatechin. The electronic density (ED) of the Lewis orbital $\pi^{(2)}_{Ci-Cj}$ and $n^{(2)}_{Oi}$ undergo a decreasing (ED < 2e) while those of the anti-Lewis orbital $\pi^{*(2)}_{Cm-Cn}$ increase (ED > 0).

These results show that intramolecular interactions are associated with the delocalization of π-elections from Lewis's orbitals to anti Lewis's orbitals. They also indicate that ring A is more stable than ring B in both molecules. The ring B is therefore more reactive than the ring A. Its reactivity influences that of the hydroxyl group O_{28}–H_{29}. $LP(O_{28})\rightarrow\pi^{*}(C_{22}-C_{24})$ transition is the most active of the $LP(O_{i})\rightarrow\pi^{*}(C_{m}-C_{n})$ transitions. Its delocalization energy (24.07 kcal/mol) is the lowest of the four catechin.

This finding is too valid for epicatechin. More, it contrasts the reactivity priority order of the hydroxyls. Its strong reactivity also enhances that of the hydroxyl O_{28}–H_{29}. Under these conditions, any electrophilic or nucleophilic attack takes place primarily and respectively on O_{28} and O_{29}. In the event of unavailability, hydroxyl O_{26}–H_{27} becomes priority; it attaches to ring B. The other two hydrox-

yls of ring A (O_{32}–H_{33} = O_{34}–H_{35}) follow in order of reactivity. Hydroxyl O_{30}–H_{31} loops the latter from the ring C. This aspect of the research leads to this article's conclusion.

4. Conclusions

The research plans to compare the reactivity of two isomers, catechin and epicatechin, using the resources of theoretical chemistry. It's carried out at the TD-DFT/B3LYP/6-31 + G(d, p) level. It's interesting in the parameters of global and local responsiveness. The MEP and the Fukui indices make it possible to specify the latter. It also harnesses the distribution of potential energy through VEDA. It contrasts the acidity. It ends with an NBO analysis. These statistics probe that epicatechin remains the more reactive compound of the two. More, the Fukui indices and the analysis of vibration energies establish that hydroxyl group reactivity of two isomers varies in the following order: O_{28}–H_{29} > O_{32}–H_{33} = O_{34}–H_{35} > O_{30}–H_{31} > O_{26}–H_{27}. In other words, the O_{28}–H_{29} site remains the least stable of all these OH. The molecular electrostatic potential confirms these results.

The acidity indicated that the hydroxyls O_{28}–H_{29}, O_{32}–H_{33}, O_{34}–H_{35} remain the most acid in the sense of Brönsted. In other words, the hydroxyl O_{28}–H_{29} the most favourable site to participate remains in anti-free radical processes. NBO analysis detected that the stabilization energies of the two isomers equal 25 81, 25.41, 24.64 kcal/mol. Besides, it presents the transition $\pi^{(2)}_{C1-C2} \rightarrow \pi^{*(2)}_{C5-C6}$, $\pi^{(2)}_{C3-C4} \rightarrow \pi^{*(2)}_{C1-C2}$, and $\pi^{(2)}_{C5-C6} \rightarrow \pi^{*(2)}_{C3-C4}$. Their energies remain equal to 25.74, 25.95, 24.71 kcal/mol for epicatechin. It appears that ring B is more reactive than A. Its reactivity reinforces that of O_{28}–H_{29}. This hydroxyl becomes the most receptive site of the catechin or epicatechin. As a result, the hydroxyls of ring A (O_{32}–H_{33} = O_{34}–H_{35}) and of ring B (O_{26}–H_{27}) follow in decreasing order to their reactivity. This research furnishes the team's next agenda.

Conflicts of Interest

The authors declare no conflicts of interest regarding the publication of this paper.

References

[1] Wang, T.-Y., Li, Q. and Bi, K.-S. (2018) Bioactive Flavonoids in Medicinal Plants: Structure, Activity and Biological Fate. *Asian Journal of Pharmaceutical Sciences*, **13**, 12-23. https://doi.org/10.1016/j.ajps.2017.08.004

[2] Terahara, N. (2015) Flavonoids in Food: A Review. *Natural Product Communications*, **10**, 521-528. https://doi.org/10.1177/1934578X1501000334

[3] Crozier, A., Jagannath, I.B. and Clifford, M.N. (2009) Dietary Phenolics: Chemistry, Bioavailability and Effects on Health. *Natural Product Reports*, **26**, 1001-1043. https://doi.org/10.1039/b802662a

[4] Assadpour, E., Jafari, S.M. and Esfanjani, A.F. (2017) Protection of Phenolic Compounds within Nanocarriers. *CAB Review*, **12**, 1-8. https://doi.org/10.1079/PAVSNNR201712057

[5] Cantos, E., Espín, J.C. and Tomás-Barberán, F.A. (2002) Varietal Differences among the Polyphenol Profiles of Seven Table Grape Cultivars Studied by LC-DAD-MS-MS. *Journal of Agricultural and Food Chemistry*, **50**, 5691-5696. https://doi.org/10.1021/jf0204102

[6] Hollman, P.C., Cassidy, A., Comte, B., Heinonen, M., Richelle, M., Richling, E., et al. (2011) The Biological Relevance of Direct Antioxidant Effects of Polyphenols for Cardiovascular Health in Humans Isn't Established. *The Journal of Nutrition*, **141**, 989S-1009S. https://doi.org/10.3945/jn.110.131490

[7] Manach, C., Mazur, A. and Scalbert, A. (2005) Polyphenols and Prevention of Cardiovascular Diseases. *Current Opinion in Lipidology*, **16**, 77-84. https://doi.org/10.1097/00041433-200502000-00013

[8] Sugihara, N., Ohnishi, M., Imamura, M. and Furuno, K. (2001) Differences in Antioxidative Efficiency of Catechins in Various Metal-Induced Lipid Peroxidations in Cultured Hepatocytes. *Journal of Health Science*, **47**, 99-106. https://doi.org/10.1248/jhs.47.99

[9] Villaño, D., Fernández-Pachón, M.S., Moyá, M.L., Troncoso, A.M. and García-Parrilla, M.C. (2007) Radical Scavenging Ability of Polyphenolic Compounds towards DPPH Free Radical. *Talanta*, **71**, 230-235. https://doi.org/10.1016/j.talanta.2006.03.050

[10] Preedy, V.R. (2012) Tea in Health and Disease Prevention. Elsevier Science and Technology Books, San Diego.

[11] Kim, H.K., Jung, J., Kang, E.Y., Gang, G., Kim, W. and Go, G.W. (2020) *Aronia melanocarpa* Reduced Adiposity via Enhanced Lipolysis in High-Fat Diet-Induced Obese Mice. *Korean Journal of Food Science and Technology*, **52**, 255-262. https://doi.org/10.9721/KJFST.2020.52.3.255

[12] Farkhondeh, T., Yazdi, H.S. and Samarghandian, S. (2019) The Protective Effects of Green Tea Catechins in the Management of Neurodegenerative Diseases: A Review. *Current Drug Discovery Technology*, **16**, 57-65. https://doi.org/10.2174/1570163815666180219115453

[13] Grzesik, M., Naparło, K., Bartosz, G. and Sadowska-Bartosz, I. (2018) Antioxidant Properties of Catechins: Comparison with Other Antioxidants. *Food Chemistry*, **241**, 480-492. https://doi.org/10.1016/j.foodchem.2017.08.117

[14] Pervin, M., Unno, K., Ohishi, T., Tanabe, H., Miyoshi, N. and Nakamura, Y. (2018) Beneficial Effects of Green Tea Catechins on Neurodegenerative Diseases. *Molecules*, **23**, Article No. 1297. https://doi.org/10.3390/molecules23061297

[15] Naponelli, V., Ramazzina, I., Lenzi, C., Bettuzzi, S. and Rizzi, F. (2017) Green Tea Catechins for Prostate Cancer Prevention: Present Achievements and Future Challenges. *Antioxidants*, **6**, Article No. 26. https://doi.org/10.3390/antiox6020026

[16] Xiang, L.P., Wang, A., Ye, J.-H., Zheng, X.-Q., Polito, C.A., Lu, J.-L., et al. (2016) Suppressive Effects of Tea Catechins on Breast Cancer. *Nutrients*, **8**, Article No. 458. https://doi.org/10.3390/nu8080458

[17] Catel-Ferreira, M., Tnani, H., Hellio, C., Cosette, P. and Lebrun, L. (2015) Antiviral Effects of Polyphenols: Development of Bio-Based Cleaning Wipes and Filters. *Journal of Virological Methods*, **212**, 1-7. https://doi.org/10.1016/j.jviromet.2014.10.008

[18] Xu, J., Xu, Z. and Zheng, W. (2017) A Review of the Antiviral Role of Green Tea Catechins. *Molecules*, **22**, Article No. 1337. https://doi.org/10.3390/molecules22081337

[19] Rietveld, A. and Wiseman, S. (2003) Antioxidant Effects of Tea: Evidence from Human Clinical Trials. *The Journal of Nutrition*, **133**, 3285S-3292S. https://doi.org/10.1093/jn/133.10.3285S

[20] D'Archivio, M., Filesi, C., Varì, R., Scazzocchio, B. and Masella, R. (2010) Bioavailability of the Polyphenols: Status and Controversies. *International Journal of Molecular Sciences*, **11**, 1321-1342. https://doi.org/10.3390/ijms11041321

[21] Pandareesh, M.D., Mythri, R.B. and Srinivas Bharath, M.M. (2015) Bioavailability of dietary Polyphenols: Factors Contributing to Their Clinical Application in CNS Diseases. *Neurochemistry International*, **89**, 198-208. https://doi.org/10.1016/j.neuint.2015.07.003

[22] Le, Z., Liu, Z., Sun, L., Liu, L. and Chen, Y. (2020) Augmenting Therapeutic Potential of Polyphenols by Hydrogen-Bonding Complexation for the Treatment of Acute Lung Inflammation. *ACS Applied Bio Materials*, **3**, 5202-5212. https://doi.org/10.1021/acsabm.0c00616

[23] Gorbatchev, M., Gorinchoy, N. and Arsene, I. (2021) Key Role of Some Specific Occupied Molecular Orbitals of Short Chain n-Alkanes in Their Surface Tension and Reaction Rate Constants with Hydroxyl Radicals: DFT Study. *International Journal of Organic Chemistry*, **11**, 1-13. https://doi.org/10.4236/ijoc.2021.111001

[24] Lee, C., Yang, W. and Parr, R.G. (1988) Development of the Cole-Salvetti Correlation-Energy Formula into a Functional of the Electron Density. *Physical Review B*, **37**, 785-789. https://doi.org/10.1103/PhysRevB.37.785

[25] Frisch, M.J., Trucks, G.W., Schlegel, H.B., Scuseria, G.E., Robb, M.A., Cheeseman, G., et al. (2009) Gaussian 09, Revision A.1. Gaussian, Inc. Wallingford.

[26] Glendening, E.D., Reed, A.E., Carpenter, J.E. and Weinhold, F. (1998) NBO Version 3.1.

[27] Fleming, I. (1976) Frontier Orbitals and Organic Chemical Reactions. John Wiley & Sons, Chichester, New York, Brisbane etc.

[28] Streitwieser, A. (2013) Molecular Orbital Theory for Organic Chemists. *Pioneers of Quantum Chemistry*, *American Chemical Society*, 275-300. https://doi.org/10.1021/bk-2013-1122.ch009

[29] Koopmans, T. (1934) Über die Zuordnung von Wellenfunktionen und Eigenwerten zu den Einzelnen Elektronen Eines Atoms. *Physica*, **1**, 104-113. https://doi.org/10.1016/S0031-8914(34)90011-2

[30] Ignaczak, A. and Gomes, J. (1996) Interaction of Halide Ions with Copper: The DFT Approach. *Chemical Physics Letters*, **257**, 609-615. https://doi.org/10.1016/0009-2614(96)00603-3

[31] Parr, R.G., Szentpály, L.V. and Liu, S. (1999) Electrophilicity Index. *Journal of the American Chemical Society*, **121**, 1922-1924. https://doi.org/10.1021/ja983494x

[32] Fukui, K., Yonezawa, T. and Shingu, H. (1952) A Molecular Orbital Theory of Reactivity in Aromatic Hydrocarbons. *The Journal of Chemical Physics*, **20**, 722-725. https://doi.org/10.1063/1.1700523

[33] Yang, W. and Mortier, W.J. (1986) The Use of Global and Local Molecular Parameters for the Analysis of the Gas-Phase Basicity of Amines. *Journal of the American Chemical Society*, **108**, 5708-5711. https://doi.org/10.1021/ja00279a008

[34] Amić, D., Stepanić, V., Lučić, B., Marković, Z. and Dimitrić Marković, J.M. (2013) PM6 Study of Free Radical Scavenging Mechanisms of Flavonoids: Why Does O-H Bond Dissociation Enthalpy Effectively Represent Free Radical Scavenging Activity? *Journal of Molecular Modeling*, **19**, 2593-2603. https://doi.org/10.1007/s00894-013-1800-5

[35] Pliego Jr., J.R. (2003) Thermodynamic Cycles and the Calculation of pK_a. *Chemical Physics Letters*, **367**, 145-149. https://doi.org/10.1016/S0009-2614(02)01686-X

[36] Pliego Jr., J. and Riveros, J.M. (2002) Gibbs Energy of Solvation of Organic Ions in Aqueous and Dimethyl Sulfoxide Solutions. *Physical Chemistry Chemical Physics*, **4**, 1622-1627. https://doi.org/10.1039/b109595a

[37] Snehalatha, M., Ravikumar, C., Hubert Joe, I., Sekar, N. and Jayakumar, V.S. (2009) Spectroscopic Analysis and DFT Calculations of a Food Additive Carmoisine. *Spectrochimica Acta Part A*: *Molecular and Biomolecular Spectroscopy*, **72**, 654-662. https://doi.org/10.1016/j.saa.2008.11.017

[38] Venkataramanan, N.S. and Suvitha, A. (2017) Structure, Electronic, Inclusion Complex Formation Behavior and Spectral Properties of Pillarplex. *Journal of Inclusion Phenomena and Macrocyclic Chemistry*, **88**, 53-67. https://doi.org/10.1007/s10847-017-0711-y

[39] Reed, A.E., Curtiss, L.A. and Weinhold, F. (1988) Intermolecular Interactions from a Natural Bond Orbital, Donor-Acceptor Viewpoint. *Chemical Reviews*, **88**, 899-926. https://doi.org/10.1021/cr00088a005

[40] Evans, J.C. (1960) The Vibrational Spectra of Phenol and Phenol-OD. *Spectrochimica Acta*, **16**, 1382-1392. https://doi.org/10.1016/S0371-1951(60)80011-2

[41] Gangadharan, R.P. and Sampath Krishnan, S. (2014) Natural Bond Orbital (NBO) Population Analysis of 1-Azanapthalene-8-ol. *Acta Physica Polonica A*, **125**, 18-22. https://doi.org/10.12693/APhysPolA.125.18

[42] Bayoumy, A.M., Ibrahim, M. and Omar, A. (2020) Mapping Molecular Electrostatic Potential (MESP) for Fulleropyrrolidine and Its Derivatives. *Optical and Quantum Electronics*, **52**, Article No. 346. https://doi.org/10.1007/s11082-020-02467-6

[43] Gross, K.C. and Seybold, P.G. (2001) Substituent Effects on the Physical Properties and pK_a of Phenol. *International Journal of Quantum Chemistry*, **85**, 569-579. https://doi.org/10.1002/qua.1525